NJC

Accepted Manuscript

This is an *Accepted Manuscript*, which has been through the Royal Society of Chemistry peer review process and has been accepted for publication.

Accepted Manuscripts are published online shortly after acceptance, before technical editing, formatting and proof reading. Using this free service, authors can make their results available to the community, in citable form, before we publish the edited article. We will replace this *Accepted Manuscript* with the edited and formatted *Advance Article* as soon as it is available.

You can find more information about *Accepted Manuscripts* in the Information for Authors.

Please note that technical editing may introduce minor changes to the text and/or graphics, which may alter content. The journal's standard Terms & Conditions and the Ethical guidelines still apply. In no event shall the Royal Society of Chemistry be held responsible for any errors or omissions in this *Accepted Manuscript* or any consequences arising from the use of any information it contains.

ROYAL SOCIETY OF CHEMISTRY

www.rsc.org/njc

NEW J CHEM RSCPublishing

ARTICLE

Enhanced Mechanical Stability and Sensitive Swelling Performance of Chitosan/yeast Hybrid Hydrogel Beads

Cite this: DOI: 10.1039/x0xx00000x

Received 00th June 2015,
Accepted 00th June 2015

DOI: 10.1039/x0xx00000x

www.rsc.org/

Diejing Feng [a], Bo Bai*, [b], Honglun Wang [b], Yourui Suo [b]

The improvement of mechanical stability of hydrogel beads is still a challenging job for future applications of chitosan hydrogels up to data. In this work, a novel and eco-friendly chitosan/yeast hybrid hydrogel bead was fabricated by facile introduction of yeast cells into chitosan matrix through alkali gelation. The formation mechanism was proposed in details and the manufactured products were characterized by Fourier transform infrared spectroscopy (FTIR) and scanning electron microscopy (SEM), respectively. The mechanical stability test showed that the impregnation of yeast cells into chitosan matrix could effectively enhance the mechanical stability of chitosan/yeast hybrid hydrogel beads under compulsory provocation of various intensities of ultrasonic waves and centrifugal forces in comparison with pure chitosan hydrogel beads. The resultant product with 40 wt% yeast content achieved the maximum swelling ratio of 31.7 g/g in distilled water. The swelling kinetics and diffusion kinetics of chitosan/yeast hybrid hydrogel beads in distilled water were investigated, too. Benefiting from the coupling effect of special crosslinked three-dimensional network structure and their ample chemical functional groups derived from their own components, chitosan/yeast hybrid hydrogel beads have manifested an acute and adjustable response to the external environmental stimuli including pH value of external solution, salt concentration, ionic valence and temperature. Especially, the distinct loading and slow-release efficiency of chitosan/yeast hybrid hydrogel beads for the humic acid as fertilizer model have been fulfilled through alternative switch of pH values. Such pH-dependent properties of the chitosan/yeast hybrid hydrogel beads are good candidates as controlled-release carrier bio-materials, which is very likely to develop a patent utilization of chitosan/yeast hybrid hydrogel beads in the future application.

1. Introduction

Chitosan is one of the basic constitutional units of the exoskeleton of crustaceans (such as crabs and shrimp) and cell walls of fungi. Owing to the abundant resources in nature, chitosan have been granted as the second most biopolymer except for cellulous. [1, 2] The commercial chitosan is mainly produced from alkaline *N*-deacetylation of chitin. The molecular structure of the chitosan possesses a linear cationic polysaccharide where distributed randomly *D*-glucosamine (deacetylated units) and *N*-acetyl-*D*-glucosamine (acetylated units) linked by *β*-(1, 4)-glycosidic bonds. [3] One primary amino group or acetamido group (C_2), two free hydroxyl groups (C_3, C_6) per-repeat unit and the flexible structure of polymer chain endow chitosan with strong functionality and wide applications in the form of chitosan hydrogels. For example, Hiroaki has developed PEG-cross-linked chitosan hydrogel films with controllable swelling and enzymatic degradation behaviors. [4] Luo has produced carboxymethyl chitosan hydrogel beads in alcohol-aqueous binary solvent for nutrient delivery applications. [5] Among various forms of chitosan hydrogels, it has been verified that the chitosan hydrogel beads are more extensively used than in the form of flakes and powders because of their easy preparation, controllable particle size, well dispersion, large surface area, porosity and plentiful functional groups. [6] Due to these attractive and outstanding properties, the chitosan hydrogel beads have been applied in water treatment, [7] drug deliver, [8] template, [9] food analysis [10] and other fields. However, on account of the irregular crosslinking points and broad distributions of chain lengths via a conventional covalent-crosslinking approach, the normal chitosan hydrogel beads lack the effective mechanism for energy dissipation, and thus exhibit

brittle, low-stretch properties and poor mechanical stability. Therefore, the large-scaled development of chitosan hydrogel beads for commercial application faces serious impediments. To overcome these defects, the crosslinking techniques using various crosslinkers such as glutaraldehyde, thiourea, ethylenediamine and epichlorohydrin have been utilized to increase mechanical strength, [11-14] but these crosslinking routes result in only a moderate enhancement and sometimes even a lower swelling performance because some amine or hydroxyl groups are involved in the crosslinking reaction. [15] Hence, the improvement of the mechanical stability of chitosan hydrogel beads is still a challenging job for future applications of chitosan hydrogels up to data. More recently, another great effort has been made and it's discovered that the impregnation of reinforcing fillers into the hydrogel matrix can effectively improve the mechanical stability. [16] Typically, inorganic fillers, such as clays, [17, 18] carbon nanotubes, [19] and graphene oxides, [20] have been dedicated in fabricating the hybrid chitosan hydrogel beads and exerted a prominently enhanced mechanical stability, which unquestionably presented a new direction for the development of chitosan hydrogel beads with highly reinforced mechanical properties.

Yeast, as a classical and ubiquitous aquatic unicellular eukaryotic microorganism, is widely used in the various industrial fields like foods, pharmaceuticals, and regenerative medicines because of its high multiplication capacity and easy artificial cultivation. [21-25] Structurally, the yeast is comprised of the cell wall, cell membrane, cytoplasm, nucleus, vacuoles and mitochondria.[26] The mass of each yeast cell consists of about 30-50% cell wall, 10-15% protein and other soluble components. [27, 28] The cell wall of yeast is composed of approximately 90% polysaccharides, mainly glucans and mannans, and the rest are a small portion of protein, chitin and lipid, which have ample functional groups such as –OH, –COOH, $–NH_2$, $–OPO_3H_2$, $–CONH_2$ and $–SO_3H$ groups on them. [29, 30] To protect the cells against the intrusion from outside and also to prevent cells from serious shrinkage, the cell wall of yeast, just like the plant epidermis, has naturally considerable tensile strength. [31] Moreover, owing to the package and protective functions derived from the cell wall of yeast, the shape of each yeast cell presents a vividly virgin hollow morphology, which can permit the passage of water molecules and help yeast cell to retain water inside because of its individually semi-permeable property of cell wall. [32] Benefiting from these unique structures of yeast cell, it is predicable hereby that such coexistence of aforementioned excellent traits makes a good reason for yeast cell to be used as ideal bio-material filler in the preparation of chitosan/yeast hybrid hydrogel beads. Specifically, the ample hydrophilic functional groups of the yeast maybe make the chemical linkages between the chitosan matrix and yeast become stronger than those with inorganic fillers, since there might form more hydrogen bonds, Van der Wals forces or electrostatic interactions. In addition, the serious shrinkage of traditionally manufactured chitosan hydrogel might be alleviated due to the reinforcement from the considerable tensile strength of yeast cell wall. More importantly, the unique spherical hollow space within the inherent yeast microbes maybe act as a mini-reservoir to accumulate more water, which is beneficial to the aggrandizement of water preservation for the chitosan-based composite hydrogel beads. However, to date, the synthesis of hybrid hydrogel materials using the yeast cell as bio-reinforcing fillers is rarely reported.

In the present paper, in view of the above statements, the chitosan/yeast hybrid hydrogel beads were firstly fabricated by impregnating yeast cells into chitosan matrix as bio-reinforcing fillers through an instantaneous gelation method. The detailed mechanisms for the formation of chitosan/yeast hybrid hydrogel beads were proposed. The structures and morphologies were characterized by Fourier transform infrared spectroscopy (FTIR) and scanning electron microscopy (SEM), respectively. The mechanical properties were also investigated by compulsory provocation of ultrasonic waves and centrifugal forces. Swelling kinetics and diffusion kinetics were also explored to study the mechanism of the swelling process and evaluate the water absorption efficiency of chitosan/yeast hybrid hydrogel beads in distilled water. The effects of pH value, salt concentrations, ionic valence and temperature of external solutions on intelligent swelling behaviors were discussed. Based on the chemical/physical properties of chitosan/yeast hybrid hydrogel beads, the beads were taken as a potential controlled-release carrier bio-material to test the loading efficiency and in vitro slow-release efficiency of humic acid under various pH stimuli. In generally, the impregnation of yeast cells into chitoan matrix not only extended the utilization of yeast cells and avoided unnecessary consumption of chitosan, but also enhanced the mechanical stability of chitosan/yeast hybrid hydrogel beads due to its multiplication capacity, readily available, inexpensive, nontoxic, hydrophilic, biocompatible and biodegradable.

2. Experimental

2.1. Materials

Yeast powder was purchased from the Angel Yeast Corp. (Wuhan, China) and was washed before use. [28] Chitosan was supplied by Sinopharm Chemical Reagent Co., Ltd. Analytic-grade sodium hydroxide (NaOH), hydrochloric acid (HCl), potassium chloride (KCl), sodium chloride (NaCl), magnesium chloride ($MgCl_2$), calcium chloride ($CaCl_2$), aluminium chloride ($AlCl_3$) and acetic acid were afforded by Xi'an Chemical Agent Crop., and used without further purification. Humic acid was provided by Tianjing Zhiyuan Chemical Reagent Co., Ltd.

2.2. Synthesis of chitosan/yeast hybrid hydrogel beads

A series of chitosan/yeast hybrid hydrogel beads with various amount of yeast were synthesized according to the following procedures: 1.5 g chitosan was dissolved in 50 mL 2% (V/V) of acetic acid solution with vigorous stirring to ensure that the chitosan was completely dissolved. Then a specific amount of yeast was immersed into the as-prepared dispersion under mechanical stirring for 1 h. Alkali gelation of the

millimetric microspheres was obtained by dropping the above chitosan solution into a 2 M sodium hydroxide solution through a 0.7 mm gauge syringe needle. The chitosan/yeast hybrid hydrogel beads were left in the NaOH solution for 2 h, filtered and washed for several times with distilled water. At last, the chitosan/yeast hybrid hydrogel beads were dried under vacuum condition at room temperature.

2.3. Materials characterization

Fourier transform infrared (FTIR) spectra of samples were recorded on a Nicolet FTIR spectrometer in the 4000-700 cm^{-1} region by using KBr wafer technique in order to study the chemical structures of the samples. The particle size and morphological characterization of the microspheres were observed by scanning electron microscope (SEM, Hitachi S-4800), and the samples were coated with platinum of 10 nm thickness to make them conductive.

2.4. Measurement of swelling ratio

The swelling of chitosan/yeast hybrid hydrogel beads was studied by conventional gravimetric method. [33] The dry samples (~0.5 g) were immersed in excessive distilled water at room temperature for 5 h to reach the swelling equilibrium. Then the swollen sample was separated from unabsorbed water by filtering through a 100-mesh sieve and drained under gravity for 5 min until no free water remained on the surface. The equilibrium swelling ratio (S_e) of chitosan/yeast hybrid hydrogel beads was determined by weighting the swollen samples and calculated using the following equation: [34]

$$S_e\ (\mathrm{g/g}) = \frac{W_{eq} - W_d}{W_d} \quad (1)$$

Where W_d (g) and W_{eq} (g) are the mass of the samples at dried state and swelling equilibrium, respectively. The effects of various pH values (3-12), temperatures (20, 30, 40, 50 and 60 ℃) and saline solutions (KCl, NaCl, $MgCl_2$, $CaCl_2$ and $AlCl_3$) on water absorbency were tested by the same methods. The measurements were performed in three replicates and average data were used for calculation of swelling ratio.

2.5. Mechanical stability test

The response of the chitosan/yeast hybrid hydrogel beads to ultrasonic waves gives an insight into the mechanical stability of the beads. Mechanical stability test was conducted as follows: certain amount of previously swelling equilibrium chitosan/yeast hybrid hydrogel beads were submerged in 100 mL distilled water using a ultrasonic processor (KH-160TDV) with a high power sonic tip operated at various20 kHz frequency (50-90 kHz) for 10 min. For another mechanical stability test, the pre-swollen chitosan/yeast hybrid hydrogel beads were centrifuged at various rotate speeds (3000-6000 rpm). The percentage of weight retention of chitosan/yeast hybrid hydrogel beads was detected from the wet weight differences of the beads before and after ultrasonication or centrifugation, respectively.

$$\text{Weight retention}\ (\%) = \frac{W}{W_e} \times 100 \quad (2)$$

Where W_e and W are the wet weights of the chitosan/yeast hybrid hydrogel beads before and after ultrasonication or centrifugation.

2.6. Humic acid loading and in vitro slow-release properties

To investigate the feasibility of using chitosan/yeast hybrid hydrogel beads as the carrier or release material for a multifunctional controlled-release fertilizer system, humic acid as a model fertilizer was loaded into the chitosan/yeast hybrid hydrogel beads with 40 wt% yeast content using swelling-diffusion method. Specifically, ~0.5 g of dried hydrogels was placed into 50 mL of 30 μg/mL humic acid solution at pH 4.5-10.5. The mixture was shaken in an incubator shaker (SHZ-82A) at 120 rpm for 30 min, and then the swollen hydrogels were separated by filtration and dried to a constant mass in a vacuum oven at 30 ℃. The concentration of the supernatant of humic acid solution was estimated at a wavelength of 254 nm using an Evolution 201 UV-vis spectrophotometer to determine the loading efficiency. [35, 36] To study the in vitro slow-release property of humic acid from chitosan/yeast hybrid hydrogel beads, the above humic acid-loaded chitosan/yeast hybrid hydrogel beads were suspended in 100 mL distilled water with different pH values (4.5-10.5), which was agitated at 120 rpm at 30 ℃. At predetermined time intervals, 3 mL release medium was withdrawn, separated by centrifugation and assayed spectrophotometrically at 254 nm. The dissolution medium was supplied with 3 mL of distilled water to keep constant volume. The loading and release efficiency of humic acid was determined by the following equations:

$$\text{Loading efficiency}\ (\%) = \frac{C_0 - C_e}{C_0} \times 100 \quad (3)$$

$$\text{Release efficiency}\ (\%) = \frac{C_r}{C_0 - C_e} \times 100 \quad (4)$$

Where C_0 (μg/mL), C_e (μg/mL) and C_r (μg/mL) are the concentrations of humic acid solutions initially, after loading and after releasing, respectively.

2.7. Statistical analysis

All data reported were the average of three repeated experiments with standard deviation of 5.0%. When the relative error exceeded 5.0%, a new experiment was performed until the relative error falls within an acceptable range. A nonlinear regression analysis by using ORIGIN 8.0 was employed to determine the values of the kinetic parameters. Basically, the nonlinear chi-square test statistic (χ^2) is the sum of the squares of the difference between the experimental data and calculated data, with each squared

difference divided by the corresponding data predicted from standard model. For a best fitted model, χ^2 will be a small number; otherwise, it will be a large number. Thus, χ^2 was used to analyze the data set to confirm the best fitted kinetic model for the adsorption.

3. Results and discussion

3.1. Preparation and characterization of chitosan/yeast hybrid hydrogel beads

A proposed mechanism for the formation of chitosan/yeast hybrid hydrogel beads by alkali gelation is shown in Scheme 1.

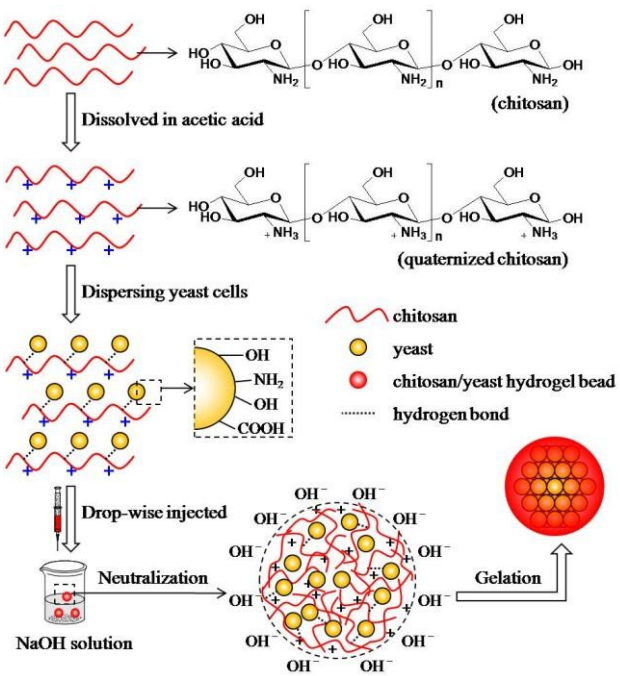

Scheme 1. Formation mechanism of chitosan/yeast hybrid hydrogel beads.

According to previous reports, chitosan belongs to a weak base and is insoluble in water, but soluble in dilute aqueous acidic solutions below its pKa (~6.3), in which the glucosamine units ($–NH_2$) of chitosan can be facilely converted into the soluble protonated form ($–NH_3^+$). [35] Hence, the chitosan presents a readily soluble performance in dilute acidic solutions at pH below 6.0. In practice, the organic acids such as acetic, formic and lactic acids are often used for dissolving chitosan. Hereinto, acetic acid is the most commonly used medium at about pH 4.0 as a reference. [37] In the current work, chitosan was dissolved in advance in 2% acetic acid solution with vigorously stirring to acquire a homogeneous quaternized chitosan solution, and thus intertwined together to form a three-dimensional network linked by hydrogen bonding or Van der Wals forces in aqueous solutions. Since the glucosamine units ($–NH_2$) derived from chitosan polymers were quaternized, the chitosan network tended to expand due to the repulsive forces among $–NH_3^+$ ions. With the subsequent introduction of yeast cells into the system, such expansion provided the great possibility for yeast cells to be uniformly dispersed and embedded into the chitosan polymer network. Thereafter, the mixture was drop-wisely injected into NaOH solution. $–NH_3^+$ groups were deprotonated, and thus the protonated chitosan polymer lost the positive charge up to a critical value of gelation. [38] In other words, the neutralization of $–NH_3^+$ sites into $–NH_2$ led to the disappearance of ionic repulsions between chitosan polymer chains, and the chitosan/yeast hybrid hydrogel beads were formed through physical cross-linking of polymer chains involving hydrogen bonds and hydrophobic interactions. [39, 40] These procedures were able to be confirmed during the synthesis by a visible alteration of morphology and shape of the chotosan/yeast solution from suspension to microspheres when the mixture drop was neutralized and gelated in alkaline solution. Relying on those multiple ways, the yeast cells could be successfully buried into the framework of chitosan hydrogels and the millimetric chitosan/yeast hybrid hydrogel beads were formed in alkaline conditions. Judging from the procedures above-mentioned, it is divinable that the obtained physical chitosan/yeast hybrid hydrogel beads should contain water, chitosan and yeast cells with free $–NH_2$ and –OH groups.

From the above analysis, it can be supposed that the chitosan polymers and yeast cells have make their own extraordinarily important contributions to the formation of chitosan/yeast hybrid hydrogel beads. Generally, chitosan polymers have play a significant bi-functional role in the formation of the chitosan/yeast composite structure. On the one hand, the native entanglement or crosslinking property of chitosan polymer chains help the discrete yeast cells reunite together tightly and become a stable three-dimensional network of the chitosan/yeast hybrid hydrogel beads due to the strong hydrogen bonding linkage. On the other hand, the inherent water absorption capacity of three-dimensional network entangled by hydrophilic chitosan polymers are still retained within the chitosan/yeast hybrid hydrogel beads, which could inevitably enhance the total water absorbency of chitosan/yeast hybrid hydrogel beads. Similarly, the yeast cells play four vital roles in the chitosan/yeast hybrid hydrogel beads. Firstly, the cell wall is composed of approximately 90% polysaccharides, mainly polymers of mannose (mannoproteins, *ca* 40% of the cell wall dry mass), polymers of glucose (β-glucan, *ca* 60% of the cell wall dry mass) and polymers of *N*-acetylglucosamine (chitin, *ca* 2% of the cell wall dry mass), [41] from which derive various hydrophilic groups, such as hydroxyl, carboxyl, amidogen, phosphate, acylamino and sulfonyl groups. The substantial functional groups on the surface of yeast cells provide an outstanding ability to anchor the chitosan polymer chains via hydrogen bonding, Van der Wals forces or electrostatic interactions, which contribute to embedding yeast cells into the framework of chitosan hydrogels tightly and firmly as well as forming a stable hybrid network structure. Secondly, the unique internal hollow shape of yeasts serves as mini-reservoir to retain absorbed water and increase the water absorbency further in

comparison with pure chitosan beads. Thirdly, the mechanical stability of pure chitosan hydrogel beads can be strengthened by filling of yeast cells into framework because of the considerable tensile strength of yeast cell wall. More importantly, the internal part of chitosan microspheres is partially replaced by cheap yeast, avoiding unnecessary waste of chitosan resource. From this point of view, the prepared chitosan/yeast hybrid hydrogel beads are demonstrated to represent a new absorbent with low cost, considerable absorption capacity, simple preparation, and practical applicability by using abundant, biodegradable and renewable traits of chitosan and yeast.

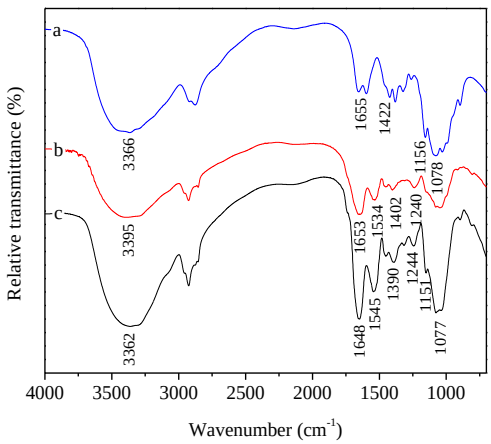

Fig.1 FTIR spectra of (a) chitosan, (b) yeast and (c) chitosan/yeast hybrid hydrogel beads.

To find possible interactions between chitosan and yeast in the formation of chitosan/yeast hybrid hydrogel beads by alkali gelation, FTIR spectroscopy was employed to monitor the transformation of chemical bonds of parallel chitosan, native yeast and chitosan/yeast hybrid hydrogel beads, as exhibited in Fig.1. For chitosan, the peaks at 3366 cm^{-1} is attributed to axial stretching vibration of O–H superimposed to the N–H stretching band and intermolecular hydrogen bonds of the polysaccharide, and the peaks at 1655 and 1422 cm^{-1} correspond to $–NH_2$ and –OH bending vibration respectively, manifesting the existence of amide and hydroxyl groups. The adsorption peaks appear as 1156 and 1078 cm^{-1} are ascribed to the asymmetric stretching of C–O–C bridge vibration and skeletal vibration involving the C–O stretching, respectively. As for yeast, the broad and strong peak observed at 3395 cm^{-1} is due to intermolecular and intramolecular hydroxyl stretching vibration. The peaks at 1653, 1534, 1402, 1240 cm^{-1} and the bands in the region of 1200−1000 cm^{-1} are assigned to C=O in amide I, N−H in amide II, C–N in amide III, C–O in carboxylic acid groups, C–O in ester groups and the stretching vibration of C–O–C ring vibrations of carbohydrates separately, which are characteristic absorption peaks of yeast. [41, 42] In the FTIR spectrum of chitosan/yeast hybrid hydrogel beads, the above characteristic absorption peaks belonging to chitosan and yeast were almost retained or even stronger. However, the bands at 3366 cm^{-1}, 1655 cm^{-1} and 1422 cm^{-1} of chitosan and 3395 cm^{-1}, 1653 cm^{-1} and 1402 cm^{-1} of yeast were shifted to 3362 cm^{-1}, 1648 cm^{-1} and 1390 cm^{-1} in chitosan/yeast hybrid hydrogel beads, respectively. Furthermore, the adsorption peak of O–H and N–H stretching vibration is much broader and more intense than single chitosan or yeast. These changes fully indicated that chitosan network and yeast cells in the chitosan/yeast hybrid hydrogel beads were intertwined together primarily via strong intermolecular hydrogen-bonding interactions between $–NH_2$ and –OH groups, and such linkage contributed to the formation of a stable three-dimensional network.

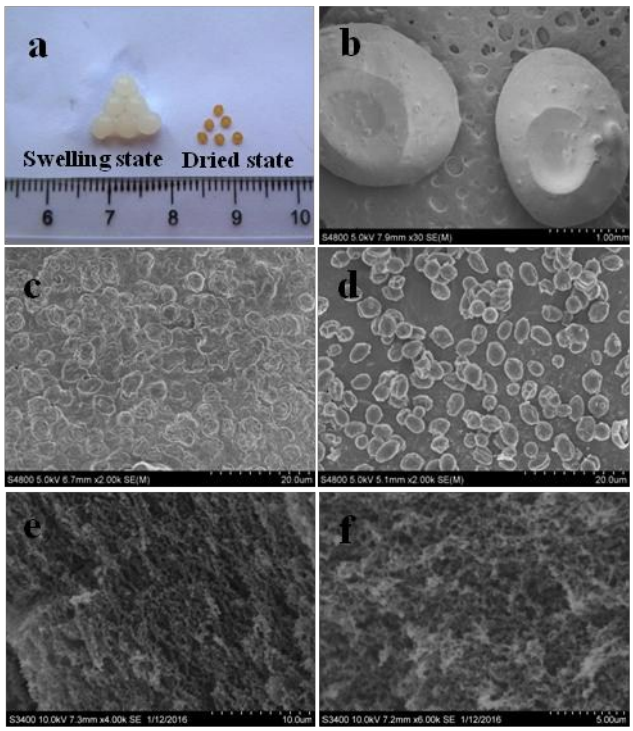

Fig.2 (a) Photographs of chitosan/yeast hybrid hydrogel beads at equilibrium swelling (left) and dried state (right), and (b) SEM micrographs of chitosan/yeast hybrid hydrogel beads, (c) the cross section of chitosan/yeast hybrid hydrogel beads, (d) native yeast cells, (e and f) SEM micrographs of chitosan in the chitosan/yeast hybrid hydrogel beads after gradient dehydration and critical point drying.

Typical photographs (a) and SEM micrographs (b-f) of chitosan/yeast hybrid hydrogel beads are presented in Fig.2, providing the information on the size and morphology. As can be seen from Fig.2a, the equilibrium swelling chitosan/yeast hybrid hydrogel beads (left) have a sphere shape and a smooth surface with mean diameter distribution about 4.0 mm, while the average diameter of dried chitosan/yeast hybrid hydrogel beads (right) is about 1.2

mm. Such enlargement of size reveals that the chitosan/yeast hybrid hydrogel beads indeed have definite absorption capacity. The theoretical water-holding capacity (WHC) of per bead can be determined from the increased diameter of particles.

$$\mathrm{WHC\ (mg)} = \rho_{\mathrm{W}} \cdot V_{\mathrm{W}} = \rho_{\mathrm{W}} \cdot \left(V_{\mathrm{eq}} - V_{\mathrm{d}}\right)$$

$$= \rho_{\mathrm{w}} \cdot \frac{4}{3}\pi\left(R_{\mathrm{eq}}^{3} - R_{\mathrm{d}}^{3}\right) \qquad (5)$$

Where ρ_{w} and V_{w} are the density and volume of the absorbed water in the chitosan/yeast hybrid hydrogel beads, respectively. V_{eq}, V_{d}, R_{eq} and R_{d} are the volume and diameter of swelling equilibrium (subscript eq) and dried (subscript d) bead samples. In this study, the water-holding capacity of per chitosan/yeast hybrid hydrogel bead was theoretically about 260.84 mg.

From the SEM micrograph of dried chitosan/yeast hybrid hydrogel beads in Fig.2b, the surface is relatively rough with small convex protrusions on it. It may be caused by the impregnation of yeast into chitosan hydrogel beads. The big depression on the surface is ascribed to severe shrinkage of chitosan/yeast hybrid hydrogel beads under absolutely drying condition. Although the network of chitosan/yeast hybrid hydrogel beads contract seriously at this moment, they still can be restored to a spherical shape, which may benefit from the stable three-dimensional network of chitosan/yeast hybrid hydrogel beads in a certain contraction range and the considerable tensile strength of yeast cells. In Fig.2c, the cross section of chitosan/yeast hybrid hydrogel beads displays a rugged plane with many yeast cells embedded in chitosan network, and the yeast microspheres still retain the original shape in contrast with their parent yeast cells in Fig.2d (ellipsoid 3.92±0.2 μm in length and 3.38±0.2 μm in width). The further careful observation shows that some yeast cells aggregate closely and deeply embedded in the crosslinked chitosan network owing to the intermolecular hydrogen bonding linkage among chitosan polymers and yeast cells. The difficulty of identifying even trace amounts of scattered yeast cells on the cross section of chitosan/yeast hybrid hydrogel beads during the half slicing processes give another evidence that the internal linkage between yeast cells and chitosan possess superior mechanical strength. In brief, stable and tight chitosan/yeast hybrid hydrogel beads were formed. Fig.2e and f presents the crosslinked chitosan network within the hybrid hydrogen beads after gradient dehydration and critical point drying. The porous structure consisted of close linked chitosan polymers. The pores with average diameter of ~0.2 μm were evenly distributed, which accords with earlier observation. [43] In this case, the arrays of hollow yeast cells interconnected by honeycomb-like polymeric structure were obtained, and the porous structure endowed the hydrogen beads with excellent absorption capacity. Thus, the chitosan/yeast hybrid hydrogel beads could perfectly integrate the properties of the two components, *i.e.*, chitosan and yeast cells, and further exert outstanding composite merits.

3.2. Enhanced Mechanical stability of chitosan/yeast hybrid hydrogel beads

The response to ultrasonic wave is an easy-going and efficient way to test mechanical stability of hydrogel beads in resistance to ultrasonic fracture, and also gives us some valuable information about mass loss and water retention for further analysis. In other word, the mechanical stability can be learned from the percentage weight loss of beads by measuring the weight difference of the beads before and after compulsive ultrasonic stimulation. [44] Thus, to assess the mechanical properties of chitosan/yeast hybrid hydrogel beads, a series of equilibrium swelling chitosan/yeast hybrid hydrogel beads with various yeast contents (0~50 wt%) were hereby dealt with the compulsory provoking of various intensity ultrasonic waves (50~90 kHz). The results are presented in Fig.3.

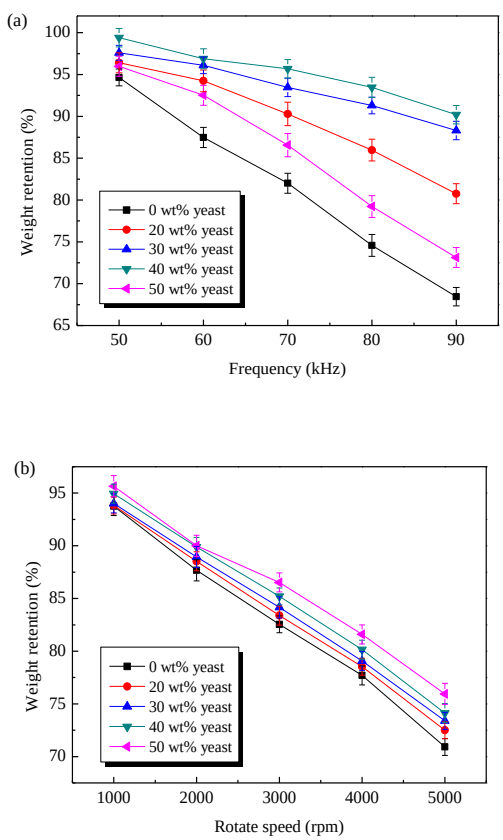

Fig.3 Mechanical stability of chitosan/yeast hybrid hydrogel beads under ultrasonication (a) and centrifugation (b).

Fig.3a displays the wet weight retention of chitosan/yeast hybrid hydrogel beads with various yeast

contents under ultrasonication. Obviously, with the increasing of the frequency of ultrasonic waves from 50 to 90 kHz, the weight retention of chitosan/yeast hybrid hydrogel beads presented a decreasing trend. At the same frequency, the beads with various yeast contents behaved different weight retention followed the sequences: 40wt% > 30 wt % > 20 wt % > 50 wt % > 0 wt %. Hereinto, the wet weight retention of the chitosan/yeast hybrid hydrogel beads filled with 20% yeast content was greatly improved as compared to the pure chitosan hydrogel beads after ultrasonication at the same frequency. The observed improvement of wet weight retention is attributed to that the interpenetration of yeast cells in the chitosan network has improved the crosslinking density of network linked by the strong hydrogen bonding interaction between the hydrophilic functional groups of yeast cells and the –OH and $–NH_2$ groups of chitosan matrix. Moreover, as the yeast content increased to 40%, the wet weight retention was increased to 93.5% under 50 kHz frequency of ultrasonic wave and the chitosan/yeast hybrid hydrogel beads still remained intact. It can be inferred that the hydrogen bonding-crosslinked network with incorporation of yeast cells could effectively withstand the ultrasonic fracture to preserve the beads in their nature state, and thus reinforce the mechanical stability of chitosan/yeast hybrid hydrogel beads. Furthermore, the unique internal hollow shape of yeast cells is able to serve as mini-reservoir for retaining absorbed water, and thus the wet weight retention can be increased with the increasing yeast content up to 40%. Whereas, as the yeast content exceeded 40%, more aggregation of yeast cells occurred, and the excess yeasts crammed the valid water absorption sites of three-dimensional network of chitosan/yeast hybrid hydrogel beads, which hindered the movement of water molecules in the network as well as the water absorption and reduced crosslinking points of three-dimensional network. Consequently, the chitosan/yeast hybrid hydrogel beads with inevitable aggregation of yeast cells were vulnerable to ultrasonic fracture and caused premature failure of impact strength of sound energy from ultrasonication. For pure chitosan hydrogel beads, they were almost single-component spheres only composed of chitosan chains without any filler or crosslinker, which had not enough resistance to bear the ultrasonic destruction. In addition, it is noteworthy that the poor stability of network may result in seriously fracture of chitosan/yeast hybrid hydrogel beads from inside to outside at higher ultrasonic frequency, and the wet weight retention decreased ineluctably as well. The same results have been reported in earlier publication. [45]

According to the literature, the centrifugal force is subject to the forcible compression forces. [46] The response of hydrogel beads to centrifugal force can be also sensitively reflected by water retaining capacity. To further confirm the mechanical stability of chitosan/yeast hybrid hydrogel beads, another test was carried out under the varied centrifugal rotate speed (1000~5000 rpm). The wet weight retention at various rotate speeds is depicted in Fig.3b. As can be seen, the wet weight retention of chitosan/yeast hybrid hydrogel beads decreased with the increasing centrifugal rotate speed from 1000 to 5000 rpm. More specifically, the wet weight retention under the same conditions of centrifugal force was increased with the increase of yeast content in the hydrogel beads, accredited to the synergy of embedded yeast cells and chitosan network. In particular, the nature toughness of yeast cell wall had a great resistance to water loss from compression forces to further prevent chitosan/yeast hybrid hydrogel beads from badly compressing under centrifugation. What's more, the three-dimensional network of chitosan/yeast hybrid hydrogel beads crosslinked by strong hydrogen bonding interaction possessed good compression resisting property, and the hydrogen bonds served as a crack bridge to remain the structure intact and stabilize the deformations of centrifugation. For example, Cong has certified that the hydrogen-bonding network of hydrogel could preserve the memory of the initial state of the hydrogel, and such intertwined network could effectively relax the locally applied stress and dissipation of the crack energy to improve the mechanical strength of hybrid hydrogels. [47]

All in all, the impregnation of yeast cells into chitosan network through intermolecular bonding interactions is an effective way to reduce water loss and enhance the mechanical stability of chitosan/yeast hybrid hydrogel beads at the same time.

3.3. Water absorbency of kinetic analysis

The development and application of chitosan/yeast hybrid hydrogel beads largely depend on the water absorbency. Analysis of the swelling kinetics of water absorbency is of great benefit to study the mechanism of the swelling process and evaluate the water absorption efficiency of chitosan/yeast hybrid hydrogel beads. Thus, the pseudo-first-order and pseudo-second-order kinetic models were adopted to fit the experimental data. The pseudo-first-order kinetic model is based on the approximation that the absorption rate relates to the quantity of unoccupied sites. The pseudo-second-order kinetic model is deduced on the basis of the concept that the absorption relates to the squared product of the difference between the number of available equilibrium absorption sites and that of occupied sites. [48] The models are expressed in the following equations: [49, 50]

$$\ln(S_e - S_t) = \ln S_e - K_1 t \quad (6)$$

$$\frac{t}{S_t} = \frac{1}{K_2 \cdot S_e^2} + \frac{t}{S_e} \quad (7)$$

Where S_e (g/g) and S_t (g/g) are the water absorbency at swelling equilibrium and at contact time t (min), and K_1 (min^{-1}) and K_2 (g/g·min) are the rate constants of the

pseudo-first-order and pseudo-second-order kinetic models, respectively. The fitting curves are exhibited in Fig.4, and the kinetic parameters and correlation coefficients are presented in Table 1.

Fig.4a plotted the variation of swelling ratio of chitosan/yeast hybrid hydrogel beads with various content of yeast as a function of swelling time. It is clear that the increase of swelling ratio was kinetically characterized by two parts, *i.e.*, the initial fast step and the asymptotical process to the equilibrium swelling ratio (S_e). It was the substantial hydrophilic groups in the chitosan/yeast hybrid hydrogel beads that help water molecules be absorbed in the network and penetrated into yeast cells to cut down the osmotic pressure difference between the internal structure and external solution. The larger osmotic pressure difference existed, the faster water molecules permeated into the absorbents. So, the synthesized chitosan/yeast hybrid hydrogel beads showed a higher velocity in premier swelling progress. As the swelling continued, more water molecules diffused into the network and gradually weakened the osmotic pressure difference. As a result of continuously overcoming the osmotic pressure inside the chitosan/yeast hybrid hydrogel beads, the swelling rate became smaller and the swelling ability finally reached equilibrium. In generally, the value of S_e varied with altering the yeast content, and the chitosan/yeast hydrogel beads of with 40% (W/W) yeast content showed an optical swelling ratio about 31.7 g/g. It can be expected that the swelling performance of pure chitosan hydrogel beads were only resulted from the entanglement of chitosan polymer chains with a high degree of crosslinking. In contrast, provided that parts of chitosan polymers were replaced with the adulterations of yeast cells, the crosslinking points of chitosan polymers might be reduced by impregnating yeast (< 40%) into chitosan hydrogel beads. Thereupon, the water molecules could facilely permeate through the crosslinked structure and gradually seep into the internal hollow cavity of yeast cells, and obviously the yeast cells have served as mini-reservoirs embedded in the hybrid hydrogels to accumulate water during their swelling processes. However, the excessive yeast content (> 40%) destroyed the crosslinked structure of chitosan polymer, and thus on this occasion the water absorption capacity of chitosan/yeast hydrogel beads were largely dependent on the physical storage traits of yeasts.

Table 1 Kinetic parameters for the water absorbency of chitosan/yeast hybrid hydrogel beads in distilled water.

yeast content	$S_{e,exp}$ (g/g)	Pseudo-first-order kinetic model				Pseudo-second-order kinetic model			
		$S_{e,cal}$ (g/g)	K_1 (min^{-1})	R^2	χ^2	$S_{e,cal}$ (g/g)	K_2 (g/g·min)	R^2	χ^2
0 wt%	26.3	21.2635	0.1189	0.9908	0.1621	28.5959	0.0082	0.9978	0.0086
20 wt%	27.8	22.7870	0.1170	0.9910	0.1532	30.1477	0.0079	0.9987	0.0044
30 wt%	29.1	21.5055	0.1048	0.9790	0.2903	31.3480	0.0081	0.9992	0.0026
40 wt%	31.7	26.0204	0.1175	0.9867	0.2297	34.1880	0.0074	0.9993	0.0018
50 wt%	30.5	23.0367	0.1035	0.9851	0.1987	32.9489	0.0073	0.9993	0.0020

As also can be seen from Table 1, the values of the correlation coefficient (R^2) of pseudo-second-order kinetic model are much closer to 1.0, and the values of chi square or the residual sum of squares (χ^2) are much closer to 0 than pseudo-first-order kinetic model, indicating that the swelling process of chitosan/yeast hybrid hydrogel beads in distilled water fit better with pseudo-second-order kinetic model than pseudo-first-order kinetic model. In addition, the $S_{e,cal}$ values as obtained from the pseudo-second-order kinetic model were much closer to the experimental data ($S_{e,exp}$) than that from the pseudo-first-order kinetic model. Therefore, the swelling process of chitosan/yeast hybrid hydrogel beads in distilled water followed the pseudo-second-order kinetic model better.

The diffusion behaviors of distilled water into chitosan/yeast hybrid hydrogel beads were further analyzed by using the empirical equation: [51]

$$\log(M_t/M_e) = \log(k) + n\log(t) \quad (8)$$

Where M_t (g/g) and M_e (g/g) are the mass of water absorbency at time t (min) and at equilibrium swelling state, separately. M_t/M_e is the fractional uptake of water normalized with respect to the equilibrium conditions. The variable k is a characteristic constant of chitosan/yeast hybrid hydrogel beads incorporating characteristics of macromolecule and penetrant system. The diffusion exponent n is in fact the key to the equation, which can be related to diffusion coefficients and the specific mode of water transport mechanism. The equation is used to account for the coupled effects of Fickian diffusion and viscoelastic relaxation in polymer systems. For spheres, a value of $n \leq 0.43$ indicates Fickian transport, $0.43 < n < 0.85$ is an indication of non-Fickian transport, $n = 0.85$ testifies Case II transport, and $n > 0.85$ predicts Super Case II transport mechanism. This equation is valid below 60% of the total equilibrium mass uptake ($M_t/M_e \leq 60\%$). [52, 53] The criteria for selecting the most appropriate model are based on the correlation coefficient (R^2). [54] From the slope and intercept of the plot of $\log(M_t/M_e)$ versus $\log(t)$, the kinetic

parameters n and k were calculated. The results are exhibited in Fig.4d and Table 2.

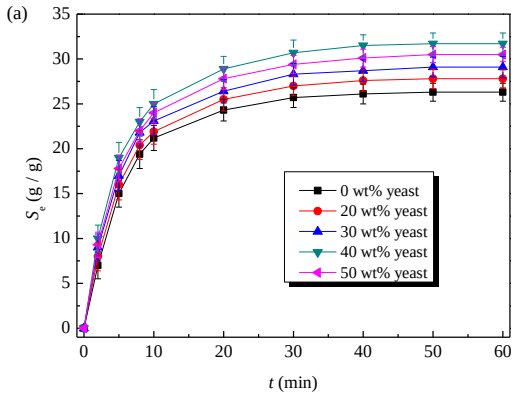

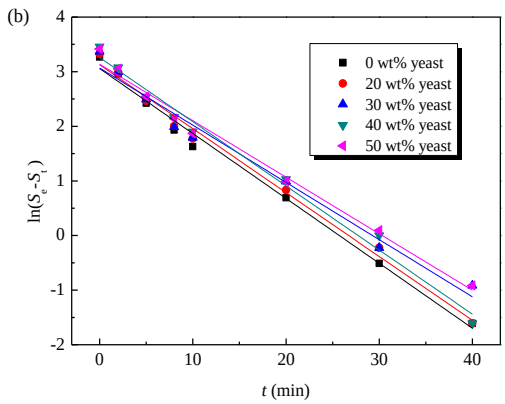

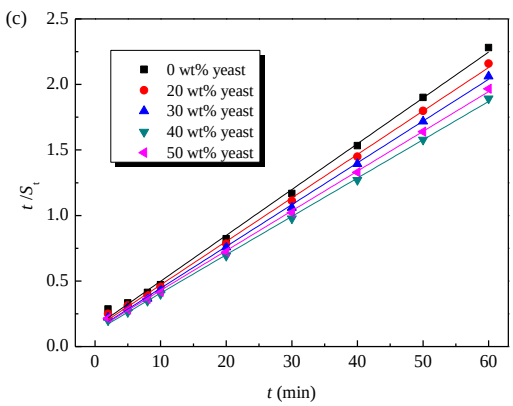

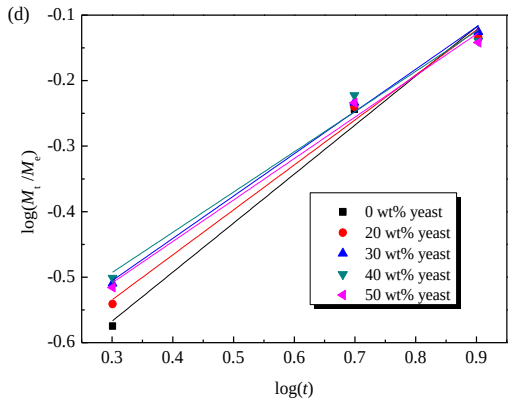

Fig.4 (a) Swelling behaviors of chitosan/yeast hybrid hydrogel beads with different yeast contents in distilled water, (b) pseudo-first-order kinetic model, (c) pseudo-second-order kinetic model and (d) diffusion kinetic in distilled water.

As can be seen from Table 2, the values of diffusion exponent (n) are in the range from 0.43 to 0.85, manifesting that the diffusion behaviors of water molecules into chitosan/yeast hybrid hydrogel beads conformed to the non-Fickian diffusion mechanism when the diffusion and relaxation rates were comparable. However, there is a general trend of decreasing values of n with increasing yeast content. For pure chitosan hydrogel beads, the water molecules were firstly diffused into the network to prompt the relaxation of chitosn chains. The diffusion rate was relatively rapid compared with the relaxation process. In this case, the rate of water diffusion was determined by the relaxation, and this restriction limited the network swelling capability. For this reason, the value of n was close to 0.85. As many more yeast cells were impregnated in the chitosan hydrogel beads, more chitosan polymers were replaced and the crosslinking points were reduced. The water molecules diffused into yeast through cell wall while the network of chitosan/yeast hybrid hydrogel beads was relaxed. The network relaxation rate was comparatively fast in contrast with the diffusion rate. In this case, the water diffusion rate played a dominant role, and thus the Fickian diffusion was relatively important. Hence, the value of n became smaller and smaller to come near to 0.43.

Table 2 Diffusion parameters and the correlation coefficient for the water diffusion of chitosan/yeast hybrid hydrogel beads in distilled water.

yeast content	n	k	R^2	χ^2	Transport mechanism
0 wt%	0.7485	0.1615	0.9821	9.49×10^{-4}	non-Fickian
20 wt%	0.6864	0.1818	0.9849	6.73×10^{-4}	non-Fickian
30 wt%	0.6458	0.1999	0.9919	3.19×10^{-4}	non-Fickian
40 wt%	0.6145	0.2102	0.9718	10.1×10^{-4}	non-Fickian
50 wt%	0.5331	0.2001	0.9795	1.19×10^{-4}	non-Fickian

3.4. Sensitive swelling behaviors of chitosan/yeast hybrid hydrogel beads

Profiting from their unique physical/chemical structure of chitosan/yeast hybrid hydrogel beads, it is predictable that the swelling behaviors of chitosan/yeast hybrid hydrogel beads should be facilely controlled by the characteristics of external solution such as pH value, salt concentrations, ionic valence and temperature.

3.4.1. Swelling behaviors at different pH values and their pulsatile behavior

In order to determine whether chitosan/yeast hybrid hydrogel beads exhibit pH sensibility, variation of water absorbency at different external buffer solutions (pH 3-12) was observed. Fig.5a depicts the swelling behaviors of chitosan/yeast hybrid hydrogel beads in solutions of various pH values adjusted by diluting HCl (pH 1.0) or NaOH (pH 10.0) solutions to avoid the influence of ionic strength. As can be seen in Fig.5a, the water absorbency is dependent on the pH values of swelling medium. With altering the pH values of swelling medium, the water absorbency was initially increased with the increase of pH to 6, and then kept almost constant in the pH range of 6-9. The further increase of pH from 10 to 12 caused a decrease of water absorbency. The water absorbency of chitosan/yeast hybrid hydrogel beads increased with the increase of yeast content from 0 to 40 wt%, and then decreased until the yeast content reached 50 wt%. The maximum swelling capacity (20.6 g/g) was obtained at pH 6 with 40 wt% yeast content. The pH-dependent swelling behaviors were due to the quaternisation of amine groups after the external pH value exceeding its pK_a (approximately 6.3), and thus the electronic repulsion between $–NH_3^+$ groups contributed the network of chitosan/yeast hybrid hydrogel beads to relaxing more. In the highly acid solutions (3 < pH < 5), the relaxation was favorable to the penetration of water molecules into the network of chitosan/yeast hybrid hydrogel beads, but the force of intermolecular and intramolecular hydrogen bonds between –OH groups was greater than the repulsive force to hinder the expansion of network. Additionally, the surface of the chitosan/yeast hybrid hydrogel beads was vulnerable to be corroded to some degree, owing to the solubility of chitosan in acidic medium. [35, 55] Thus, the network of chitosan/yeast hybrid hydrogel beads was decomposed, leading to the reduction of water absorbency. The shrinkage of the network in basic environment (10 < pH < 12) was mainly ascribed to the neutralization and charge screening effect by excess OH^-, the high osmotic pressure caused by Na^+ ions in swelling medium and the hydrogen bonds between –OH or $–NH_2$ groups. At neutral pH, the water absorption of chitosan/yeast hybrid hydrogel beads with various yeast contents was in the following order: 40% > 50% > 30% > 20% > 0%, which was in accordance with the phenomena of the water absorption in distilled water. It was largely dependent on the synergetic traits of chitosan matrix and yeast cells. As a result of continuously overcoming the osmotic pressure, the water molecules could trippingly penetrate the crosslinked structure and gradually permeate into the internal hollow cavity of yeast cells. Nevertheless, the excessive yeast content (> 40%) destroyed the crosslinked structure of chitosan matrix, and thus the water absorption ability of chitosan/yeast hydrogel beads was declined inevitably.

Analysis of swelling kinetics was also conducted in Supporting Information to evaluate the mechanism of water absorbing process into chitosan/yeast hybrid hydrogel beads with 40% yeast content. Since the chitosan/yeast hybrid hydrogel beads showed different swelling behaviors at various pH values, the pH-reversibility of chitosan/yeast hybrid hydrogel beads with 40% yeast content in the buffer solutions alternatively conducted at pH 6 and 10 was studied in Fig.5b. As can be seen, the pH-dependence occurs reversibly and relatively fast. At pH 6, chitosan/yeast hybrid hydrogel beads swelled up to 17.3 g/g in 20 minutes due to the repulsive electrostatic force of quaternized amine groups and the hydrogen bonds between hydroxyl groups and water molecules, while, at pH 10, the hydrogels shrunk as a result of the neutralization of $–NH_3^+$ groups, the high osmotic pressure and the hydrogen bonds between –OH or $–NH_2$ groups. After three on-off cycles, the chitosan/yeast hybrid hydrogel beads still had better response to environment pH stimulants, suggesting that the chitosan/yeast hybrid hydrogel beads processed excellent pH reversibility. The swelling mechanism of the pulsatile behaviors of chitosan/yeast hybrid hydrogel beads was different from that of anionic hydrogels. [56]

3.4.2. Swelling behaviors in various salt solutions

The effect of various salt solutions (0.1 mmol/L) on water absorbency of chitosan/yeast hybrid hydrogel beads was explored in Fig.5c. The water absorbency of chitosan/yeast hybrid hydrogel beads in saline solutions was distinctly declined in comparison with that in distilled water in Fig.4a. The well-known phenomenon was commonly observed in the swelling of ionic hydrogels. [55] As shown in Fig.5c, the order of swelling capacity in the chloride salt solutions was KCl > NaCl > $MgCl_2$ > $CaCl_2$ > $AlCl_3$. It can be revealed by that the multivalent metal cations could form complexes with the hydrogen groups groups of the chitosan/yeast hybrid hydrogel beads, which led to the enhancement of crosslinking density and the increase of ionic strength of saline solutions. When the crosslinking density or the ionic strength of saline solutions increased, the water absorbency decreased.

To achieve a comparative measure of sensitivity of chitosan/yeast hybrid hydrogel beads to various kinds of aqueous fluid, a dimensionless salt sensitivity factor (f) for 0.1 mmol/L salt solution was calculated by using Eq.(9): [57]

$$f = 1 - \frac{S_g}{S_d} \quad (9)$$

Where S_g (g/g) and S_d (g/g) are the equilibrium water absorbency in a given fluid and in destilled water, respectively.

The effect of the ionic strength on the water absorbency can be expressed by Flory's equation as follows: [58]

$$S^{5/3} \approx \frac{\left(i/2V_u \cdot I^{1/2}\right)^2 + (1/2 - x_1)/V_1}{v_e/V_0} \quad (10)$$

Where S is water absorbency, i/V_u is the charge density of polymer, I is the ionic strength of solution, $(1/2-x_1)/V_1$ is the polymer-solvent affinity, and v_e/V_0 is the crosslinking density.

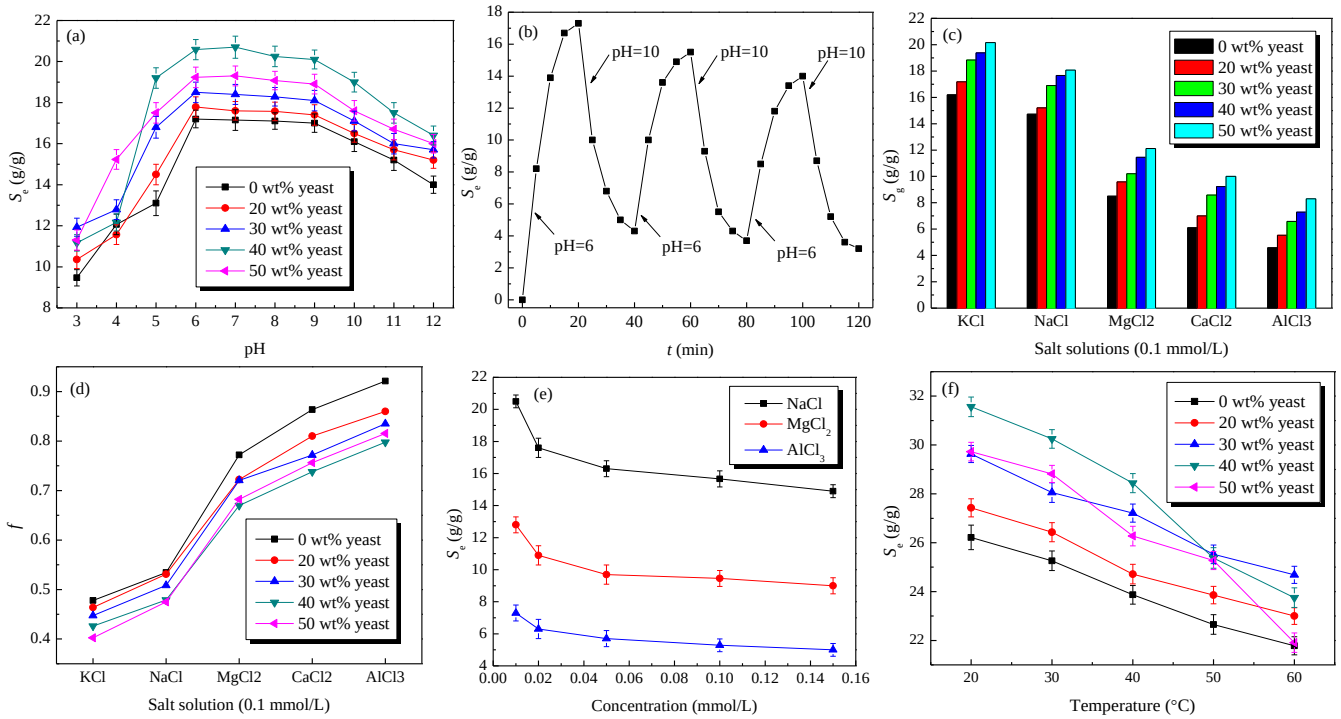

Fig.5 (a) Effect of pH on the swelling behaviors of chitosan/yeast hybrid hydrogel beads; (b) the pulsatile behavior of chitosan/yeast hybrid hydrogel beads with 40 wt% yeast content at pH 6 and pH 10 at 25 ℃; (c) effect of various salt solutions (0.1 mmol/L) on water absorbency of chitosan/yeast hybrid hydrogel beads; (d) salt sensitivity factors (f) of various saline solutions; (e) effect of various salt concentrations on the equilibrium swelling ratio of chitosan/yeast hybrid hydrogel beads with 40 wt% yeast content and (f) effect of temperature on the water absorbency of chitosan/yeast hybrid hydrogel beads.

The variations of the dimensionless salt sensitivity factor (f) with the type of salt solutions are given in Fig.5d. The value of f increased with increasing in charge of the cations (*i.e.*, monovalent > divalent > trivalent cations). The higher f values became, the higher salt sensitivity was observed. Otherwise, the larger the radius of monovalent metal cations, the greater was the water absorbency (K^+ > Na^+), and the less the radius of the same polyvalent monatomic cations, the larger the water absorbency (Mg^{2+} > Ca^{2+}). Hence, the sensitivity of the chitosan/yeast hybrid hydrogel beads to various cations was $K^+ < Na^+ < Mg^{2+} < Ca^{2+} < Al^{3+}$ at a concentration of 0.1 mmol/L. The results were in accordance with Zhang's research. [48]

Fig.5e shows the effect of various salt concentrations on the equilibrium swelling ratio of chitosan/yeast hybrid hydrogel beads with 40 wt% yeast content. It is obvious that the water absorbency decreased with increasing the concentration of external salt solutions, and the equilibrium swelling ratio in $MgCl_2$ and $AlCl_3$ solutions was lower than that in NaCl solution, even at a higher concentration. As we know, the sensitivity of chitosan/yeast hybrid hydrogel beads to monovalent saline was mainly attributed to the reduction of osmotic pressure difference between the interior of hydrogels and the external solution. The charge screening effect of cations was another factor that influenced the equilibrium swelling ratio in saline solutions. In multivalent saline solution, Mg^{2+} and Al^{3+} cations could form inter and intramolecular complexes with hydroxyl groups in chitosan/yeast hybrid hydrogel beads, which reduced the valid hydrophilic sites in polymeric chains and

produced denser crosslinked network. As a result, the rigid hydrogels were restricted to expanding the polymer network and the water-holding capability was remarkably decreased. Therefore, the combination of osmotic pressure difference and the charge screening effect determined the swelling behaviors of chitosan/yeast hybrid hydrogel beads in the given saline solution of various concentrations.

3.4.3. Swelling behaviors at different temperatures

Fig.5f shows the influence of temperature on the water absorbency of chitosan/yeast hybrid hydrogel beads in distilled water. The swelling ratio was decreased with increasing temperature of swelling bath. Otherwise, at lower temperature (20−40 ºC), the water absorbency of chitosan/yeast hybrid hydrogel beads with more yeast content was obviously higher than that u yeast content, and at higher temperature (50−60 ºC), the water absorbency plunged obviously. It was attributed to the fact that the hydrogen bonds fractured and meanwhile both the segmental mobility and diffusion of water molecules into yeast cells increased on raising the yeast content at lower temperature, leading to the enhanced water absorbency. However, with further increasing the temperature to 60 ℃, the yeast embedded in the chitosan hydrogels begun to shrink due to that the yeast cell wall was out of activity and so the water absorbency of chitosan/yeast hybrid hydrogel beads with high yeast content (40~50 wt%) was inferior to that with low yeast content (0~30 wt%). This proved that the yeast served as water storage tank in chitosan/yeast hybrid hydrogel beads, and it was entirely feasible to take yeast as a promising filling biomaterial to boost the water absorbency of hydrogels.

3.5. Application of chitosan/yeast hybrid hydrogel beads for Humic acid loading and in vitro slow-release

Humic acid is commonly used as a soil supplement in agriculture. As an organic matter soil amendment, humic acid has been widely known by farmers to be beneficial to plant growth. Previous researches have indicated that the addition of humate to soil significantly increased root mass in creeping bentgrass turf. [59, 60] Another study on the effects of humic acid on plant growth was conducted at Ohio State University which said in part “humic acids increased plant growth” and that there were “relatively large responses at low application rates”. [61] In reality, humic acids behave as mixtures of dibasic acids, with a pK_1 value around 4 for protonation of carboxyl groups and around 8 for protonation of phenolate groups. There is considerable overall similarity among individual humic acids. [62] Specifically, so-called "gray humic acids" (GHA) are soluble in low-ionic-strength alkaline media; "brown humic acids" (BHA) are soluble in alkaline conditions independent of ionic strength; and fulvic acids (FA) are soluble independent of pH and ionic strength. [63] By this token, it seems that the future application of humic acid is in reliance on its usage ways obviously and extremely. Therefore, to find a simple mode for the controllable-use of humic acid in practice becomes an urgent job. In the subsequent study, an exemplified study of loading efficiency and in vitro slow-releasing efficiency of humic acid was investigated elaborately by taking chitosan/yeast hybrid hydrogel beads as a potential controlled-release carrier bio-material.

The effect of pH on loading efficiency of humic acid into chitosan/yeast hybrid hydrogel beads with 40 wt% yeast content is represented in Fig.6a. The loading behavior of humic acid closely relied on the swelling properties of chitosan/yeast hybrid hydrogel beads. The loading curves exhibited a typical sustained swelling mode consisting of an initial absorption followed by a plateau. There was large amount of humic acid adsorbed into chitosan/yeast hybrid hydrogel beads at pH 4.5–6.5 while less humic acid was loaded with increase of pH from 7.5 to 10.5 remarkably. The maximum loading efficiency was 81.4% at pH 5.5. It can be explained that the $–NH_2$ groups derived from chitosan/yeast hybrid hydrogel beads and –COOH groups of humic acid were differently affected by weak acid conditions. The resulting electrostatic repulsion between the protonated $–NH_3^+$ groups weakened the intermolecular and intramolecular hydrogen bonding interaction, and loosed network structure to facilitate the diffusion of humic acid into chitosan/yeast hybrid hydrogel beads. Synchronously, the electrostatic force of $–NH_3^+…–COO^-$ pairs led to a splendid loading efficiency, which was similar to previous study. [64] As time went by, the cationic groups became less, and thus the loading efficiency reached equilibrium within 35 min. We can infer from the above that the more acidic external medium is the more vulnerable chitosan/yeast hybrid hydrogel beads are to acid corrosion. Therefore, the external environment at pH 5.5 could prevent the chitosan/yeast hybrid hydrogel beads from being seriously eroded.

The in vitro slow-release efficiency of humic acid from chitosan/yeast hybrid hydrogel beads with 40 wt% yeast content is shown in Fig.6b. According to the results, it can be concluded that the slow-release efficiency was strongly depended on pH values of incubation medium. In comparison with loading, the slow-release efficiency of humic acid at pH 7.5-10.5 was superior to that at pH 4.5-6.5. The optical in vitro slow-release efficiency of humic acid was 82.6% at pH 7.5. As the protonated $–NH_3^+$ groups were deprotonated in alkaline condition, considerable humic acid was leased from chitosan/yeast hybrid hydrogel beads. The higher pH value of incubation medium was, the more $–NH_3^+$ groups were deprotonated, but withal the strong hydrogen bonds between chitosan/yeast hybrid hydrogel beads and humic acid would dominate the release efficiency. Due to the hydrogen bonding between $–NH_2$

groups or –OH groups, a relatively dense network structure was formed which largely restricted the release of humic acid. Additionally, the swelling of chitosan/yeast hybrid hydrogel beads could affect the release properties as well. The slow-release of humic acid lasted about 300 min. It should be noted that the slow-release efficiency cannot reach 100%, since some humic acid molecules might be tangled through the network and those cannot be released unless the polymer matrices of chitosan/yeast hybrid hydrogel beads are degraded.

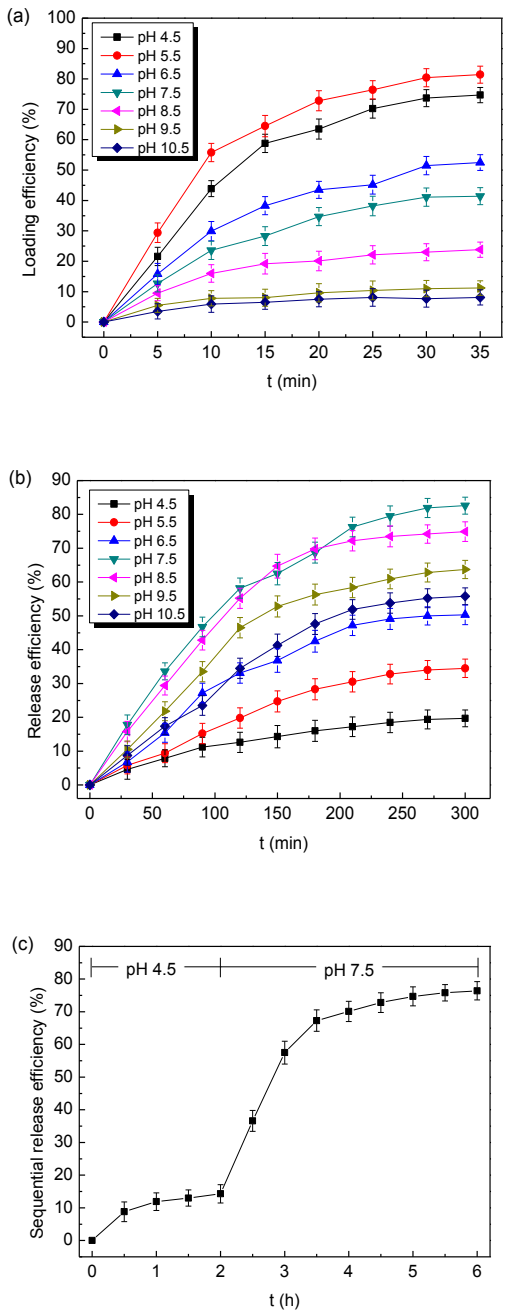

Fig.6 (a) The effect of pH on loading efficiency of humic acid into chitosan/yeast hybrid hydrogel beads, (b) the effect of pH on in vitro slow-release efficiency of humic acid from chitosan/yeast hybrid hydrogel beads and (c) the stepwise controlled-release behavior of humic acid from chitosan/yeast hybrid hydrogel beads at pH 4.5 and 7.5.

In consequence of the pH-dependent release behaviors, dried chitosan/yeast hybrid hydrogel beads loaded with humic acid were immersed in a solution with a pH value of 4.5 for initial 2 h and subsequently in a solution of pH 7.5 at 30 ℃. The sequential controlled-release profiles of chitosan/yeast hybrid hydrogel beads in response to a stepwise change in pH values of external medium was revealed in Fig.6c. The sequential release efficiency of humic acid at pH 4.5 was 14.3% within 2 h. With incremental pH value from 4.5 to 7.5, the sequential release efficiency had a dramatic step change and reached approximately 76.4%. Also, the release time to equilibrium at pH 7.5 was twice the time at pH 4.5. This stepwise controlled-release behavior of humic acid clear showed the versatility of chitosan/yeast hybrid hydrogel beads to respond to the sequential change of pH values of external solutions. Therefore, the chitosan/yeast hybrid hydrogel beads are good candidates as controlled-release carrier materials, which develop a novel application of chitosan/yeast hybrid hydrogel beads.

4. Conclusions

In conclusion, we have successfully proposed a facile approach to prepare the eco-friendly chitosan/yeast hybrid hydrogel beads with various yeast contents by alkali gelation. The formation mechanism was proposed in details. The impregnation of yeast into chitosan hydrogel beads not only could improve the mechanical stability of chitosan/yeast hybrid hydrogel beads to prevent their severe shrinkage under the forcible ultrasonication or centrifugation, but also exhibit enhanced absorption capacity than that of pure chitosan hydrogel beads. The resultant product with 40 wt% yeast content achieved the maximum swelling ratio of 31.7 g/g in distilled water. The swelling process of chitosan/yeast hybrid hydrogel beads in distilled water fitted better with pseudo-second-order kinetic model than pseudo-first-order kinetic model, and the diffusion behaviors conformed to the non-Fickian diffusion mechanism. Due to the special structure and the functional groups, chitosan/yeast hybrid hydrogel beads responded to a variety of environmental stimuli including pH value of external solution, salt concentrations, ionic valence and temperature, and show different swelling ratio. Moreover, the chitosan/yeast hybrid hydrogel beads exhibited distinct loading and slow-release efficiency of humic acid at various pH values. Such pH-dependent chitosan/yeast hybrid hydrogel beads are good candidates as controlled-release carrier materials, which develops a novel application of chitosan/yeast hybrid hydrogel beads in the future application.

Acknowledgements
This work was supported by Shaanxi Provincial Natural Science Foundation of China (No.2015JM2071), and Fundamental Research Funds for the Central Universities (No. 310829162014).

Notes and references

[a] College of Environmental Science and Engineering, Chang'an University, Xi'an, 710054, P.R. China.
[b] Key Laboratory of Tibetan Medicine Research, Northwest Institute of Plateau Biology, Chinese Academy of Sciences, Xining, 810001, P.R. China.
Fax: +86 29 82339961;
Tel: +86 29 82339052;
E-mail: baibochina@163.com (Bo Bai)

1. A.A.Yaşar and D.A. Nuran, Chem. Eng. J., 2009, **151**, 188.
2. K.A.A. Pereira, L.R. Osório, M.P. Silva, K.S. Sousa, E.C.D.S. Filho, Materials Research, 2014, **17**, 141.
3. E. Campos, P. Coimbra and M.H. Gil, Polym. Bull., 2013, **70**, 549.
4. H. Tanuma, T. Saito, K. Nishikawa, T. Dong, K. Yazawa and Y. Inoue, Carbohydr. Polym., 2010, **80**, 260.
5. Y. Luo, Z. Teng, X. Wang and Q. Wang, Food Hydrocolloid., 2012, **31**, 332.
6. A.J. Varma, S.V. Deshpande and J.F. Kennedy, Carbohydr. Polym., 2004, **55**, 77.
7. Q. Peng, M. Liu, J. Zheng and C. Zhou, Micropor. Mesopor. Mat., 2015, **201**, 190.
8. M. Yadollahi, S. Farhoudian and H. Namazi, Int. J. Biol. Macromol., 2015, **79**, 37.
9. R. Jiang, H.Y. Zhu, H.H. Chen, J. Yao, Y.Q. Fu, Z.Y. Zhang and Y.M. Xu, Appl. Surf. Sci., 2014, **319**, 189.
10. H. Zhao, N. Li, J. Li, X. Qiao and Z. Xu, Food Anal. Method., 2015, **8**, 1363.
11. G.Crini, Prog. Polym. Sci., 2005, **30**, 38.
12. L. Zhou, Y. Wang, Z. Liu and Q. Huang, J. Hazard. Mater., 2009, **161**, 995.
13. J.S. Wang, R.T. Peng, J.H. Yang, Y.C. Liu and X.J. Hu, Carbohyd. Polym., 2011, **84**, 1169.
14. G. Crini, Bioresour. Technol., 2006, **97**, 1061.
15. L. Martinez, F.B. Agnely, J. Siepmann, M. Cotte, S. Geiger and G. Couarraze, J. Pharm. Biopharm., 2007, **67**, 339.
16. C. Spagnol, F.H.A. Rodrigues, A.G.B. Pereira, A.R. Fajardo, A.F. Rubira and E.C. Muniz, Carbohyd. Polym., 2012, **87**, 2038.
17. S. Chatterjee, D.S. Lee, M.W. Lee and S.H. Woo, Bioresour. Technol., 2009, **100**, 2803.
18. M. Pathavuth and S. Punnama, Appl. Clay Sci., 2009, **42**, 427.
19. H.A. Shawky, A.H.M. El-Aassar and D.E. Abo-Zeid, J. Appl. Polym. Sci., 2012, **125**, E93.
20. L. Fan, C. Luo, S. Min, X. Li, F. Lu and H. Qiu, Bioresour. Technol., 2012, **114**, 703.
21. W. He, J.J. Cui, Y.Z. Yue, X.D. Zhang, X. Xia, H. Liu and S.W. Lui, J. Colloid Interface Sci., 2011, **354**, 109.
22. Q.W. Dai, W. Zhang, F.Q. Dong, Y.L. Zhao and X.L. Wu, Chem. Eng. J., 2014, **249**, 226.
23. Y. Goksungur, S. Uren and U. Guvenc, Bioresour. Technol., 2005, **96**, 103.
24. R.P. Han, H.K. Li, Y.H. Li, J.H. Zhang, H.J. Xiao and J. Shi, J. Hazard. Mater., 2006, **137**, 1569.
25. X.B. Yang, G.J. Jin, Z.W. Gong, H.W. Shen, Y.H. Song, F.W. Bai and Z.B.K. Zhao, Bioresour. Technol., 2014, **158**, 383.
26. F.M. Klis, Yeast, 1994, **10**, 851.
27. T.H. Nguyen, G.H. Fleet and P.L. Rogers, Appl. Microbiol. Biotechnol., 1998, **50**, 206.
28. D.J. Feng, B. Bai, C.X. Ding, H.L. Wang and Y.R. Suo, Ind. Eng. Chem. Res., 2014, **53**, 12760.
29. P. Magnelli, J.F. Cipollo and C. Abeijon, Anal. Biochem., 2002, **301**, 136.
30. C.M. Hogan, Abiotic factor. In Encyclopedia of Earth; Monosson, E., Cleveland, C., Eds.; National Council for Science and the Environment: Washington, DC, 2010.
31. N.C. Carpita, Plant Physiol., 1985, **79**, 485.
32. E.P. Feofilova, Microbiology, 2010, **79**, 711.
33. B. Bolto, T. Tran, M. Hoang and Z.L. Xie, Prog. Polym. Sci., 2009, **34**, 969.
34. M.V. Dinu, M.M. Perju and E.S. Dragan, React. Funct. Polym., 2011, **71**, 881.

35. U.V. Gaikwad and S.A. Pande, Int. Res. J. of Science and Engineering, 2013, **1**, 13.
36. S.S. Kavurmaci, M. Bekbolet, Desalin. Water Treat., 2014, **52**, 1903.
37. N.V. Toan and Hanh, T.T. J. Biotechnol., 2013, **12**, 382.
38. M. Dasha and F. Chiellinia, Prog. Polym. Sci., 2011, **36**, 981.
39. S. Ladet, L. David and A. Domard, Nature, 2008, **452**, 76.
40. A. Montembault, C. Viton and A. Domard, Biomaterials, 2005, **26**, 933.
41. J.J. Cui, W. He, H.T. Liu, S.J. Liao and Y.Z. Yue, Colloids Surf., B, 2009, **74**, 274.
42. W. He, Z.M. Li, Y.J. Wang, X.F. Chen, X.D. Zhang and H.S. Zhao, J. Mater. Sci.-Mater. Med., 2010, **21**, 155.
43. D. Kowalczyk, M. Kordowska-Wiater, J. Nowak and B. Baraniak, Int. J. Biol. Macromol., 2015, **77**, 350.
44. S. Chatterjee, T. Chatterjee, and S.H. Woo, Bioresour. Technol., 2010, **101**, 3853.
45. T. Jiang, T. Kuila, N.H. Kim, B.C. Ku, J.H. Lee, Compos. Sci. Technol., 2013, **79**, 115.
46. Y. Delmotte and J. Diorio, Fibrin material and method for producing and using the same. United States Patent 6,965,014 B1. 2005-11-15.
47. H. Cong, P. Wang and S. Yu, Small, 2014, **10**, 448.
48. M. Zhang, Z. Cheng, T. Zhao, M. Liu, M. Hu and J. Li, J. Agr. Food Chem., 2014, **62**, 8867.
49. M. Evren, I. Acar, K. Guclu and G. Guclu, Can. J. Chem. Eng., 2014, **92**, 52.
50. T. Singh and R. Singhal, J. Appl. Polym. Sci., 2013, **129**, 3126.
51. J.R. Witono, I.W. Noordergraaf, H.J. Heeres and L.P.B.M. Janssen, Carbohyd. Polym., 2014, **103**, 325.
52. P.L. Ritger and N.A. Peppas, J. Control. Release, 1987, **5**, 23.
53. N.A. Peppas, Pharm. Acta. Helv., 1985, **60**, 110.
54. P. Costa and J.M. Sousa Lobo, Eur. J. Pharm. Sci., 2001, **13**, 123.
55. L. Liu, J.P. Yang, X.J. Ju, R. Xie, Y.M. Liu, W. Wang, J.J. Zhang, C.H. Niu and L.Y. Chu, Soft Matter, 2011, **7**, 4821.
56. E. Akar, A. Altınışık and Y. Seki, Carbohyd. Polym., 2012, **90**, 1634.
57. A. Pourjavadi, S. Barzegar and G.R. Mahdavinia, Carbohyd. Polym., 2006, **66**, 386.
58. Y. Bao, J. Ma and N. Li, Carbohyd. Polym., 2011, **84**, 76.
59. R.J. Cooper, C. Liu and D.S. Fisher, Crop Sci., 1998, **38**, 1639.
60. C. Liu, R.J. Cooper and D.C. Bowman, Hortscience, 1998, **33**, 1023.
61. N.Q. Arancon, C.A. Edwards, S. Lee and R. Byrne, Eur. J. Soil. Biol., 2006, **42**, S65.
62. E.A. Ghabbour and G. Davies, Humic Substances: Structures, Models and Functions. RSC, Cambridge, U.K. 2001, 141-156, ISBN 978-0-85404-811-3.
63. R. Baigorri, M. Fuentes, G. González-Gaitano, J.M. García-Mina, G. Almendros and F.J. González-Vila, J. Agr. Food. Chem., 2009, **57**, 3266.
64. A. Jebali, A. Behzadi, I. Rezapor, T. Jasemizad, S.H. Hekmatimoghaddam, G.H. Halvani and N. Sedighi, Int. J. Environ. Sci. Te., 2015, **12**, 45.

Graphical Abstract